Mineralized microbes from Giggenbach submarine volcano

Brian Jones,[1] C. E. J. de Ronde,[2] and Robin W. Renaut[3]

Received 5 November 2007; revised 11 March 2008; accepted 14 April 2008; published 24 July 2008.

[1] The Giggenbach submarine volcano, which forms part of the Kermadec active arc front, is located ~780 km NNE of the North Island of New Zealand. Samples collected from chimneys associated with seafloor hydrothermal vents on this volcano, at a depth of 160–180 m, contain silicified microbes and microbes entombed in reticular Fe-rich precipitates. The mineralized biota includes filamentous, rod-shaped, and rare coccoid microbes. In the absence of organic carbon for rDNA analysis or preserved cells, the taxonomic affinity of these microbes, in terms of extant taxa, remains questionable because of their architectural simplicity and the paucity of taxonomically significant features. The three-dimensional preservation of the microbes indicates rapid mineralization with a steady supply of supersaturated fluids to the nucleation sites present on the surfaces of the microbes. The mineralization styles evident in the microbes from the Giggenbach submarine volcano are similar to those associated with mineralized microbes found in terrestrial hot spring deposits in New Zealand, Iceland, Yellowstone, and Kenya. These similarities exist even though the microbes are probably different and the fluids become supersaturated with respect to opal-A by different mechanisms. For ancient rocks it means that interpretations of the depositional settings cannot be based solely on the silicified microbes or their style of silicification.

Citation: Jones, B., C. E. J. de Ronde, and R. W. Renaut (2008), Mineralized microbes from Giggenbach submarine volcano, *J. Geophys. Res.*, *113*, B08S05, doi:10.1029/2007JB005482.

1. Introduction

[2] Microbes, irrespective of where they live, commonly act as templates for the nucleation and precipitation of opal-A and other minerals because of the reactive sites that exist on their surfaces [e.g., *Ferris et al.*, 1986; *Urrutia and Beveridge*, 1994; *Schultze-Lam et al.*, 1995; *Fortin and Beveridge*, 1997]. Although the microbes are generally assumed to play a passive role in opal-A precipitation [*White et al.*, 1956; *Konhauser et al.*, 1993; *Phoenix et al.*, 2003; *Yee et al.*, 2003], there are indications that some microbes may exert some control over the initial coatings of opal-A [*Jones et al.*, 2004a, 2004b]. Microbial mineralization is commonly associated with hydrothermal waters that emerge from vents located on land [*Weed*, 1890], on lake floors [*Remsen et al.*, 1990], and on the seafloor in shallow [*Canet et al.*, 2005] or deep [*Stüben et al.*, 1994; *Halbach et al.*, 2002] water settings.

[3] Silicification of microbes around terrestrial hot springs and oceanic vents takes place in significantly different environments, even though both are fed by thermal waters that circulate in the shallow upper crust. Subaerial silicification around terrestrial hot springs takes place at atmospheric pressure, usually in well-illuminated conditions (except at high latitudes such as Iceland) where water temperature, pH, and mineral saturation levels are influenced by ambient air temperatures and the influx of rainwater. In stark contrast, microbial silicification around most seafloor vents takes place in relatively high-pressure, typically dark environs where water temperature, pH, and saturation levels are influenced primarily by the degree of mixing of the silica-laden hydrothermal fluid with ambient (cold) seawater. By comparing silicified microbes from these different settings it should be possible to determine if the environmental setting plays any role in microbial silicification and hence, add to the debate regarding the role that microbes may play in their own silicification.

[4] Giggenbach volcano, located ~780 km NNE of the North Island of New Zealand, is one of numerous submarine volcanoes along the Kermadec arc (Figure 1a) that discharge hydrothermal fluids into the surrounding oceans [*de Ronde et al.*, 2001, 2007], and is part of the much larger convergent plate boundary that marks the "Pacific Ring of Fire" [*de Ronde et al.*, 2003]. Giggenbach is a simple volcanic cone that rises about 1000 m from the seafloor and has a ~1-km-wide crater at its summit which in turn has a small, ~100-m-high cone in the center that rises to within 80 m of the sea surface (Figure 1b). A hydrothermal system, hosted in its summit, is dominated by diffuse, relatively low temperature ($\leq$200°C) venting. Evidence for focused venting is given by numerous, inactive, 1- to 2-m-tall chimney structures (see below) which, in contrast to the high-temperature (~300°C),

[1]Department of Earth and Atmospheric Sciences, University of Alberta, Edmonton, Alberta, Canada.
[2]GNS Science, Lower Hutt, New Zealand.
[3]Department of Geological Sciences, University of Saskatchewan, Saskatoon, Saskatchewan, Canada.

0148-0227/08/2007JB005482$09.00

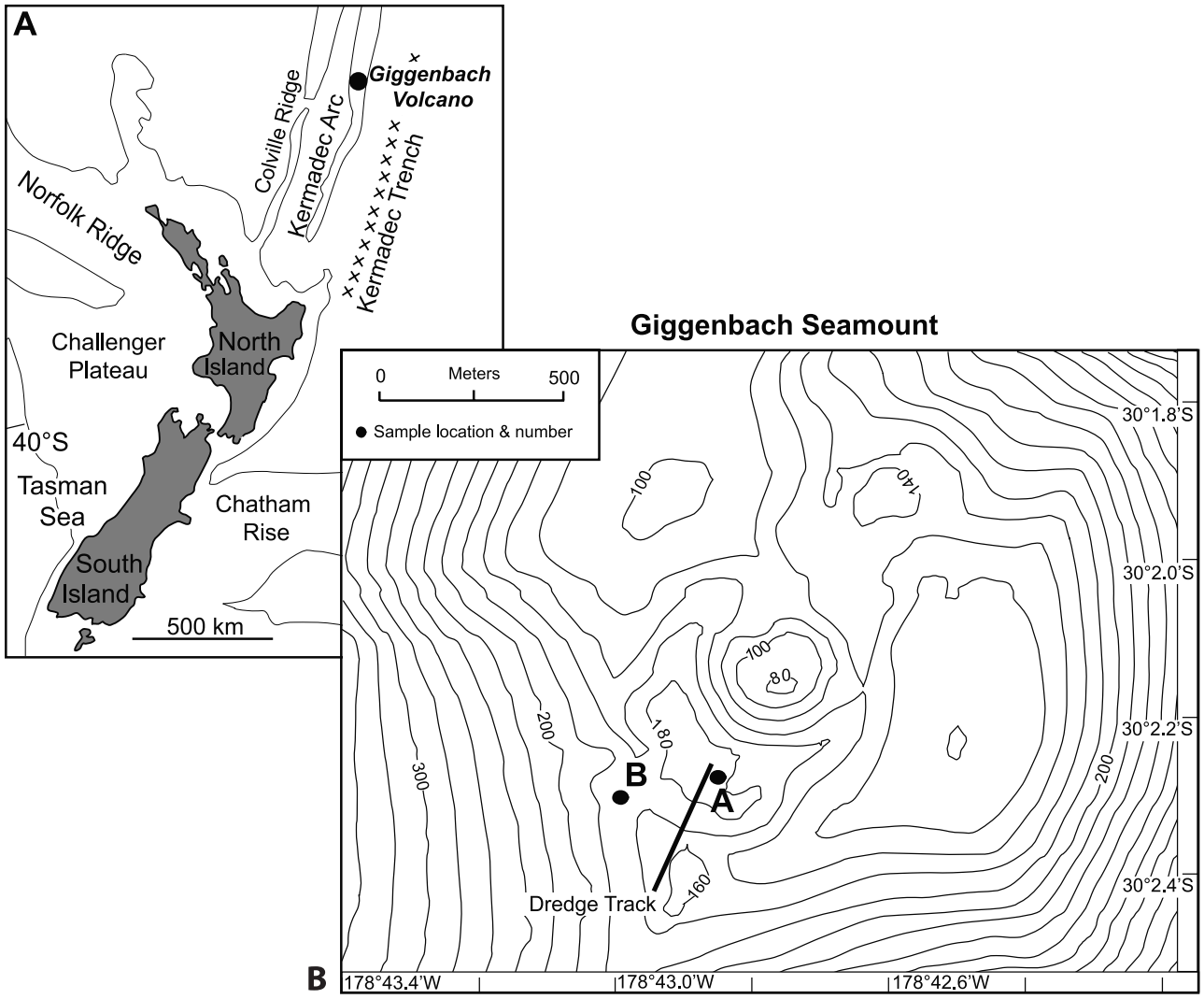

Figure 1. Location maps. (a) Location of Giggenbach submarine volcano. (b) Bathymetric map of Giggenbach showing localities A (30°02.251′S, 178°42.836′W), B (30°02.297′S, 178°42.994′W), and C which was collected along the indicated dredge line (start at 30°02.309′S, 178°42.843′W, end at 30°02.411′S, 178°42.930′W).

metal-rich chimneys seen elsewhere along the arc (e.g., Brothers volcano [*de Ronde et al.*, 2005]), are composed mainly of silica.

[5] This paper is based on three samples collected from localities A, B, and C that are at depths of 180–190 m on the Giggenbach volcano (Figure 1b). The samples from localities A and B were collected by the deep diving submersible *Pisces V* during the April–May 2005 NZAS-RoF cruise, with the R/V *Ka'imikai-o-Kanaloa*. The precise location of locality C is unknown because the sample was dredged from the south side of the volcano summit during the May 2002 NZAPLUME II cruise while aboard the R/V *Tangaroa* [*de Ronde et al.*, 2007]. The dredge started in a water depth of ~162 m, suggesting that it was near the rim of the summit crater (Figure 1b). This study focuses primarily on silicified microbes found in these samples. After describing and illustrating their morphology, assessing their biogenicity, and determining their pattern of mineralization, these silicified marine microbes are compared with silicified microbes found in terrestrial spring deposits. These comparisons provide a basis for assessing the role that environmental settings play in microbial silicification.

2. Methodology

[6] Small fractured pieces, broken from each sample, were mounted on stubs and sputter coated with a very thin layer of gold before being examined on a JOEL 6301FE scanning electron microscope (SEM) at an accelerating voltage of 5 kV. This study is based mostly on the 325 SEM photomicrographs that were taken from these samples. Mineral identification relied on the morphology of the precipitates and elemental analyses as determined from energy dispersive X-ray (EDX) analysis on the SEM that

were conducted with an accelerating voltage of 20 kV. The small sample size precluded XRD analysis.

[7] Adobe Photoshop CS2 © was used to enhance the contrast and brightness of the underwater digital images and SEM photomicrographs used in this study.

3. Samples

3.1. Sample From Locality A

[8] This sample, from a depth of 183 m (see Figure 1b), represents the uppermost 15 cm of a silica chimney, of which there were many in this general area (Figure 2a). Figure 2b shows the ~2-m-tall chimney from which this sample was collected. This sample is composed mainly of silica and has a mostly black, translucent interior, with some whiter patches included. The chimney interior is filled with silica, apart from scattered pores, ~1 mm in diameter. Rare pyrite grains are present in the sample and a ~1-mm-thick crust of Fe-oxide occurs on the exterior surface of the sample. Relatively isolated diffuse vents are seen in the general summit crater area, where this sample was collected, especially in the southern and eastern parts (e.g., Figure 2c).

[9] The mineralized microbial mats in this sample are formed of at least three types of microbes (Figure 3). Long, small-diameter filamentous microbes (Figures 3a–3g) are common whereas rod-shaped microbes (Figures 3h–3l) are found locally. Coccoid microbes are widely scattered throughout the sample.

[10] The filamentous microbes are >20 μm long with a diameter of 0.5–1.0 μm (Figures 3a–3e). Although many microbes are apparent only as hollow tubes (Figures 3b and 3d), walls <0.1 μm thick and possible septa (Figures 3c and 3d) are present in some specimens. The preservation style is highly variable, even among filaments lying close together. Thus, some filaments are ensheathed by layers of featureless opal-A that are up to 40 μm thick (Figures 3b, 3d, and 3e), whereas others are decorated with opal-A spheres up to 0.4 μm in diameter (Figures 3h and 3i). In some areas, the silicified filaments were subsequently encased by individual and merged opal-A spheres that are up to 3 μm in diameter (Figures 3h and 3i).

[11] Rod-shaped microbes are up to 5 μm long with an external diameter of ~1 μm (Figures 3j–3l). Transverse cross sections through some filaments show that they have an open lumen encased by a wall, ~0.25 μm thick, that is formed of two thin layers of opal-A (Figure 3k). Some rod-shaped microbes appear to have been crushed between the larger opal-A spheres (Figure 3l).

[12] EDX analysis indicates that the silicified microbes are formed largely of Si and O as no other elements were detected. Locally, small clusters of acicular crystals up to 10 μm long and 0.3 μm wide are formed of As and S. Elsewhere, small blade-shaped barite crystals are present.

3.2. Sample From Locality B

[13] This locality, ~250 m west of locality A, is at a depth of 164 m (Figure 1b). The sample is a ~2-cm-thick crust rich in Fe oxides and silica. Diffuse venting nearby at marker 10 reached temperatures of ~72°C (see Figure 2c). The exterior of the sample was covered by what appeared to be mostly Mn, underlain by orange colored Fe-rich silica. The ~5-mm-thick interior contained whitish material that was interlayered with apple green colored layers. Both were soft and spongy to the touch immediately after recovery. Indeed, water could be squeezed from the sample. This sample is very similar to that collected 3 years earlier at the nearby locality "C."

[14] Sample B consists of an orange crust that is overlain by a white crust. The orange and white crusts were examined separately so that the types of microbes and composition of each crust could be ascertained.

3.2.1. Orange Crust

[15] The orange crust is a microbial mat formed of densely interwoven filamentous microbes each of which are >1 mm long with an external diameter of ~2 μm (Figures 4a–4f). The mineralized core (Figure 4d) or open lumen (Figure 4f), which may represent the diameter of the original microbe, is 0.15–0.45 μm in diameter. Although some microbes appear to branch, thick mineral precipitates commonly mask the filaments and make it impossible to determine if they are true branches or merely two filaments crossing one another (e.g., Figure 4c). There are no indications of sheathes or septa.

[16] The filaments are coated with a reticulate precipitate (Figures 4d–4f) that is commonly more compact in the cores than in the peripheral regions (Figure 4f). EDX analyses of numerous spots show that these coatings are composed mainly of Fe and Si with a trace of Mg. Variations in the peak heights on the EDX scan suggest that the amount of Fe, Si, and Mg is highly variable on a microscale.

3.2.2. White Crust

[17] The white crust is a microbial mat formed of filamentous microbes that are either interwoven or lie parallel to each other (Figures 4g–4i). The mats are difficult to delineate accurately because they are commonly hidden beneath opal-A precipitates (Figures 4g–4l). Although there may be more than one type of microbe in the white crust, long, straight, branching microbes that lie parallel to each other dominate (Figures 4h and 4i). These filaments are

Figure 2. Underwater photographs of silica-rich chimneys on Giggenbach volcano taken from the deep diving submersible *Pisces V*. (a) Alignment of Fe-silica-rich chimneys on the east side of the central cone that has grown from the center of the summit crater, at a similar depth to locality B. (b) Tall (~2 m) silica-rich chimney with two smaller chimneys in background. Sample A was broken off from the upper part of the chimney shown in foreground, at a depth of 183 m. (c) Photograph of typical diffuse venting on the south side of volcano summit, immediately south of the cone, at *Pisces V* marker 10. Maximum temperature recorded for venting here was 72.3°C. The white material is mostly bacterial mat; the yellowish material is elemental sulfur. Some vent-related mussels can be seen near the vent site. Sample C was collected from this same general area.

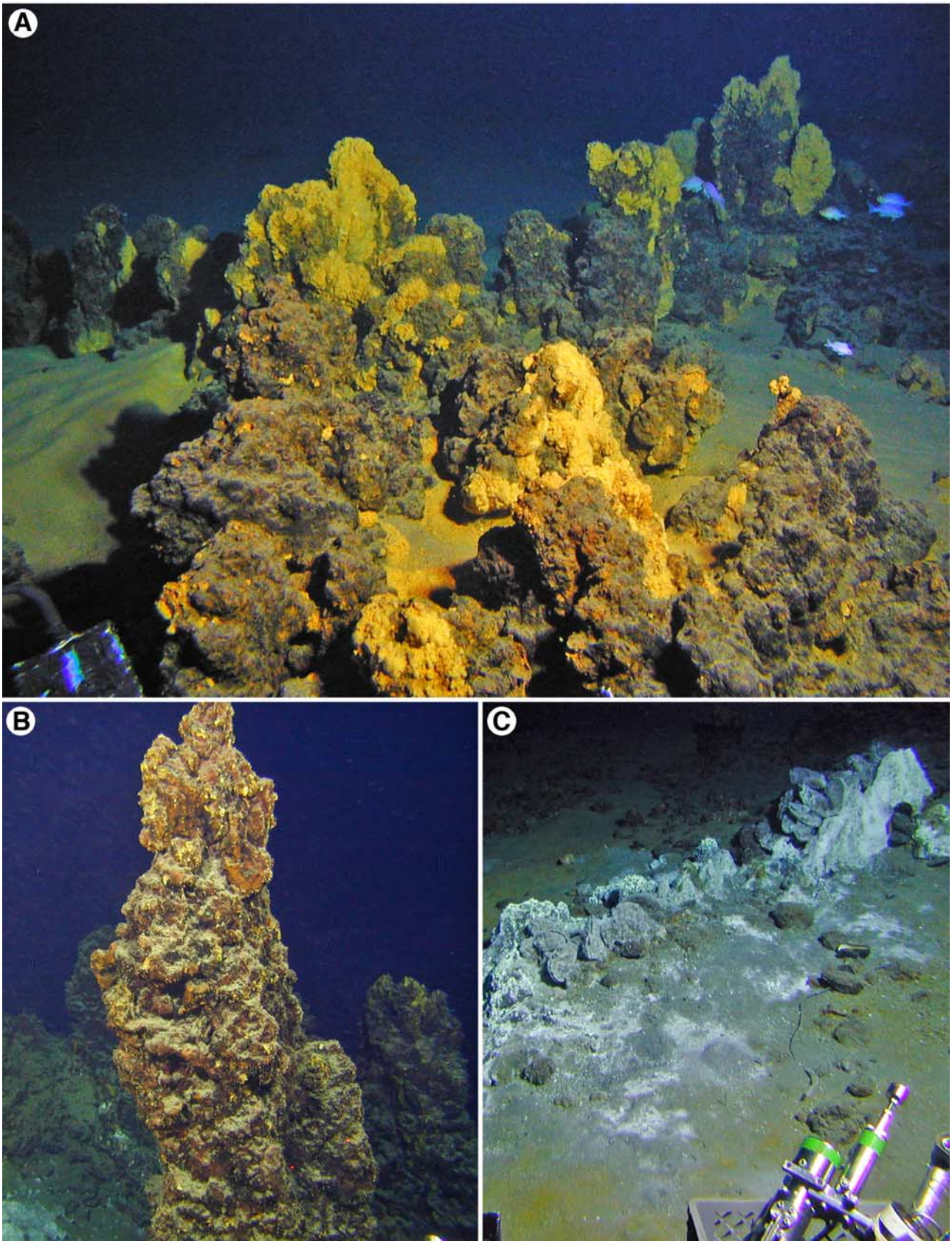

Figure 2

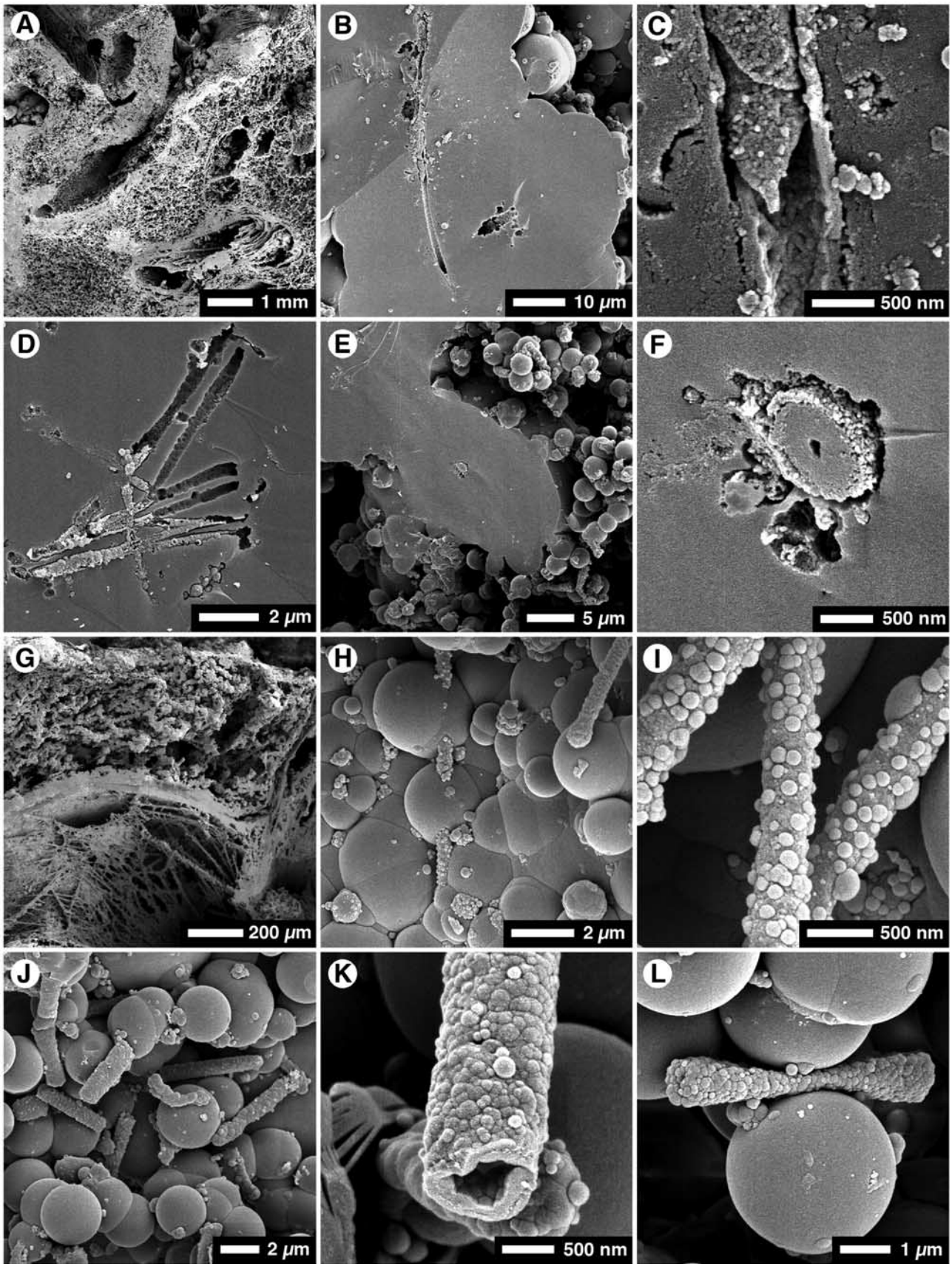
A
1 mm
B
10 μm
C
500 nm
D
2 μm
E
5 μm
F
500 nm
G
200 μm
H
2 μm
I
500 nm
J
2 μm
K
500 nm
L
1 μm

Figure 3

>5 μm long, up to 0.75 μm in diameter, and commonly appear to branch (Figure 4i). The filaments are typically hollow with walls ~0.1 μm thick and open lumens ~0.5 μm in diameter (Figures 4j–4l). The walls of the microbes are formed of featureless opal-A (Figure 4i). The exteriors of the silicified microbes are adorned with spheres of opal-A up to 0.4 μm in diameter (Figure 4i). Locally, small clusters of merged opal-A spheres completely encase the silicified filaments (Figures 4g–4i).

[18] Intermixed with the long, straight branching filaments are clusters formed of silicified microbes that exhibit complex branching patterns (Figures 4j and 4k). Their diameter and wall structure, however, is similar to that of the straight filaments (Figure 4l).

3.3. Sample From Locality C

[19] Material dredged during this transect included hydrothermally altered volcaniclastic material, dominated by fist-sized pieces of pumice which was locally mineralized by pyrite and clays. Some of this material was steaming when recovered on deck; temperatures up to 54°C were measured by inserting a temperature probe into the most highly altered material. A large (~14 cm long) black, squat looking vent-related mussel was also retrieved. Pronounced colloidal, or agate-like features characterized the sample of silica sinter found among the dredged material. Red fibrous material seen in a cavity inside the crust was thought to be 'organic'. Locally, the mostly white silica crust had an apple green coloration.

[20] This sample from locality A is formed of silicified microbial mats and thin intercalated layers (<1 mm thick) of solid, featureless opal-A (Figure 5a). At least two types of mineralized microbes are present in the silicified mats. Filamentous microbes, >250 μm long with an external diameter up to 25 μm (Figures 5a–5e), dominate the silicified microbial mats. Transverse cross sections through these filaments generally show no structures other than open lumens that are up to 2 μm in diameter (Figure 5d and 5e). The possibility that the filaments may branch is difficult to verify because the thick encrusting opal-A effectively disguises them.

[21] In some areas of the microbial mats there are distinctive microbial structures that have their outer wall preserved and/or Fe-rich reticulate coatings (Figures 5f–5l). The microbes are encased by opal-A that is up to 15 μm thick (Figures 5e–5g). These microbes have an external diameter <55 μm, walls 1–2 μm thick, and an open lumen 15–20 μm in diameter (Figures 5f–5i). The walls, which commonly appear to be formed of two layers, are composed primarily of opal-A and, in some specimens, minor amounts of Fe. Other microbial tubes of similar size lack the well-defined walls. They are, however, commonly lined with a Fe-rich reticulate coating that also contains S and locally, traces of Mg, Na, K, and Ca (Figures 5k and 5l). Small (<10 μm) pyrite framboids are locally associated with the Fe-rich reticulate coatings. It is unclear, however, if the opal-A and/or reticulate Fe-rich coating replaced the sheath and/or cell wall of the original microbe, or if these precipitates are a cement that coated the walls of the tube that formed after the organic materials of the original microbe had decayed.

4. Biogenic or Abiogenic Origin?

[22] DNA analyses of the samples produced inconclusive results (M. Stott, personal communication, 2008). Thus, the biogenicity of the microbe-like structures (Figures 3–5) in samples A, B, and C could be debated [cf. *Reysenbach and Cady*, 2001; *García-Ruiz et al.*, 2002, 2003; *Little et al.*, 2004]. This question is pertinent given that *García-Ruiz et al.* [2003] experimentally precipitated abiogenic witherite (barium carbonate) with a filamentous appearance that appeared to mimic filamentous microbes.

[23] Under conditions of high supersaturation, opal-A may precipitate homogeneously as nanospheres and microspheres in the water column, or may form heterogeneously on a solid substrate under lower levels of saturation [*Iler*, 1979]. In each case, the opal-A will usually precipitate as solid, internally laminated microspheres. The filamentous, rod-shaped, and coccoid structures preserved in the opal-A deposits from the Giggenbach seamount are considered to be biogenic because (1) abiogenic opal-A precipitation produces microspheres, not filamentous, rod-shaped, or coccoid masses, (2) different morphologies (e.g., filamentous, rod-shaped) are present in the same sample, (3) each morphotype is consistent in terms of size and shape, (4) some contain features that appear to represent septa (Figures 3b and 3c), sheaths (Figure 3f), and/or double walls (Figures 4h and 4i), (5) it is difficult to explain how an isodiametric, hollow tube could develop inside linked and intergrown abiogenically precipitated opal-A microspheres given the manner in which opal-A is normally precipitated from a fluid, (6) some of the rod-shaped structures (Figures 3j–3l) are discrete and significantly smaller than the opal-A microspheres that surround them, and (7) structures within the opal-A clearly show that they must have originally been precipitated

Figure 3. SEM photomicrographs of silicified microbes, sample A from depth of ~180 m (Figure 1b). (a) General view of silicified microbial mats. (b) Cross section through silicified microbe showing small-diameter microbe encased by thick layer of opal-A. (c) Enlarged view of small-diameter filamentous microbe, from Figure 3b, showing thin wall, and possible microbial cells. (d) Group of small-diameter filaments embedded in opal-A. (e) Cross section through opal-A mass showing small-diameter filamentous microbe in core. Note small opal-A spheres on outer surface. (f) Enlarged view of small-diameter filamentous microbe from core of opal-A mass shown in Figure 3e. (g) General view of silicified filamentous microbes and opal-A sheets. (h) Mammilated opal-A substrate with small-diameter rod-shaped silicified microbes resting on surface. (i) Silicified rod-shaped microbes coated with opal-A and scattered opal-A spheres. (j) Silicified rod-shaped microbes resting on mammilated opal-A substrate. (k) Silicified rod-shaped microbe showing thin wall around open lumen and small opal-A spheres on outer surface. (l) Silicified rod-shaped microbes sandwiched between opal-A spheres. Distortion of microbe indicates that it was crushed between the two opal-A spheres.

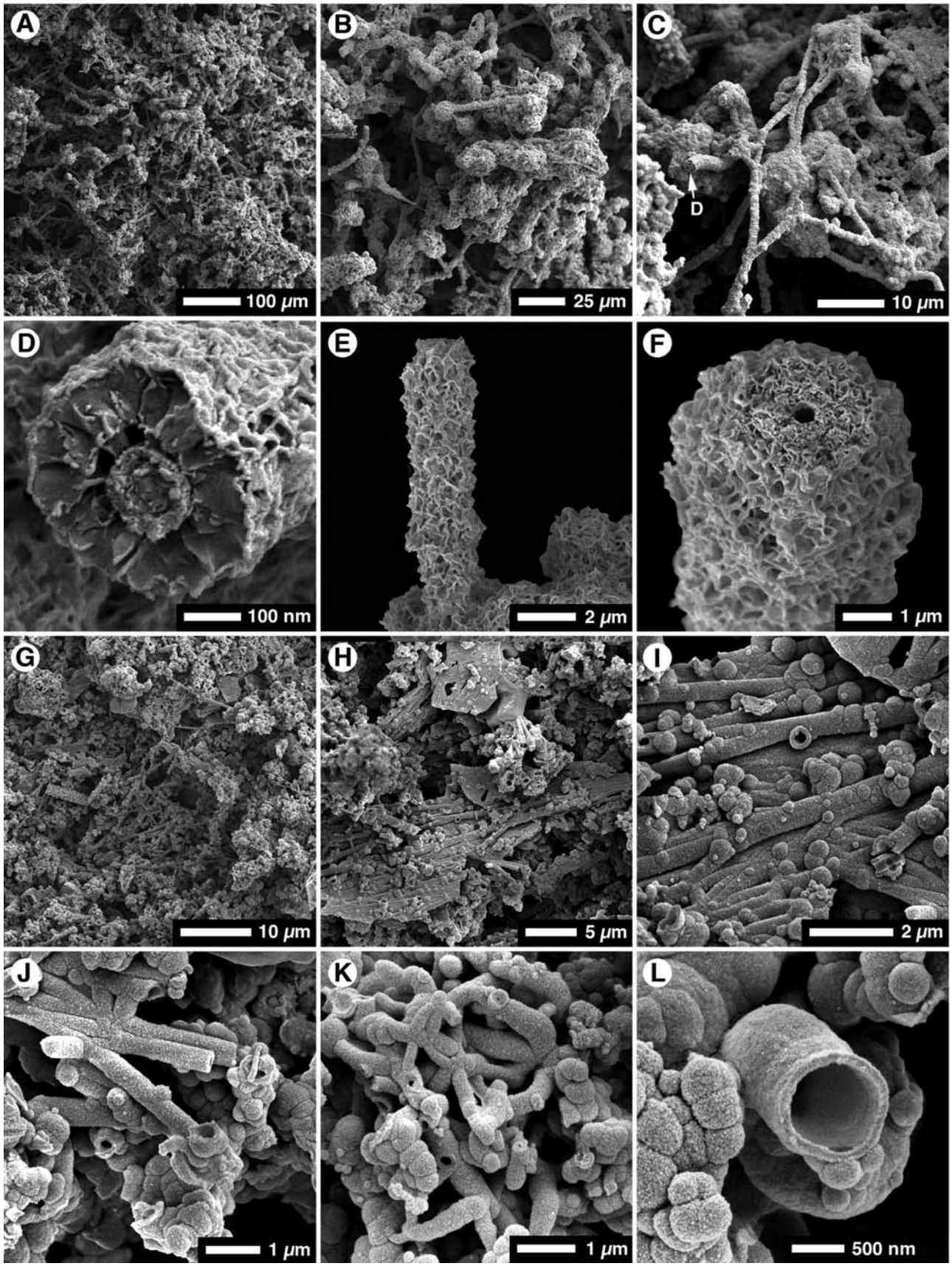
A
100 μm
B
25 μm
C
D
10 μm
D
100 nm
E
2 μm
F
1 μm
G
10 μm
H
5 μm
I
2 μm
J
1 μm
K
1 μm
L
500 nm

Figure 4

heterogeneously around a solid substrate (Figures 3i and 5i). Furthermore, the microbe-like structures evident in the opal-A from the Giggenbach seamount are similar to silicified microbes found in terrestrial geyser and hot spring systems [e.g., *Jones et al.*, 1997].

[24] Despite the lack of organic components, the morphological evidence derived from the silicified structures clearly points to a biogenic origin.

5. Microbe Affinities

[25] Solely on the basis of morphology, the biota in the samples includes the following morphotypes:

[26] 1. Morphotype A consists of long, branching filamentous microbes, preserved in opal-A, that are <1 μm in diameter, with a thin (0.1–0.2 μm) wall, and an open lumen (Figures 3a-3d, 4g–4j, and 5a–5d). One specimen from locality B shows that they may be septate (Figure 3c).

[27] 2. Morphotype B consists of long, branching(?) filamentous microbes replaced and encased by reticulate Fe-rich precipitates in locality A that are >1 mm long, with an external diameter of ~2 μm, and a mineralized core or open lumen 0.15–0.45 μm in diameter (Figures 4c–4e). There are no indications of a sheath or septa. The differences between this microbe and morphotype A may reflect differences in mineralization rather than true taxonomic variance.

[28] 3. Morphotype C consists of rod-shaped microbes, <5 μm long, ~1 μm in diameter, and a wall (~250 nm thick) that encases an open lumen (Figures 3j–3l).

[29] 4. Morphotype D consists of long filamentous microbes with an external diameter <55 μm, walls 1–2 μm thick, and open lumen 15–20 μm in diameter (Figures 5f–5i). The molds of the microbes are commonly lined with Fe-rich reticulate coatings (Figures 5k and 5l).

[30] Differences in the morphology and size of the mineralized microbes indicate that more than one taxon is present in the biota. Determining the taxonomic affinities of these mineralized microbes, however, is virtually impossible because they are architecturally simple, lack organic carbon from which DNA could be extracted, and lack any distinctive morphological features of taxonomic value [cf. *Jones et al.*, 2001c, 2004b]. Moreover, the taxonomic status of many microbes found around seafloor vents is in a state of flux. Some taxa, including *Leptothrix* and *Gallionella*, have been identified by their morphology and association with Fe oxides [e.g., *Bogdanov et al.*, 1997; *Boyd and Scott*, 2001] but have yet to be characterized by DNA molecular analysis. Conversely, recent rDNA analyses are providing more information about the microbes found around submarine vents [e.g., *Emerson et al.*, 2007] but little or no information is being provided about the morphologies of the microbes from which the rDNA originated. Such diametrically opposed approaches to the characterization of these microbes makes it virtually impossible to ally mineralized microbes with extant taxa.

6. Comparison With Other Mineralized Microbes Associated With Seafloor Hydrothermal Vents

[31] Filamentous structures, which have been allied to filamentous microbes, have been found in Si and Mn-rich Fe oxides and oxyhydroxides, Fe silicates, metal sulfides, nontronite, jasper, and chert deposits associated with modern hydrothermal vents on the floors of the Pacific Ocean, the Indian Ocean, the Atlantic Ocean, and the Mediterranean [*Little et al.*, 2004, Table 1]. Specific examples include those found in the Mariana Trough in the west Pacific Ocean [*Stüben et al.*, 1994], the Galapagos Spreading Center [*Herzig et al.*, 1988], the Magic Mountain hydrothermal deposit on the Southern Explorer Ridge in the northeast Pacific Ocean [*Fortin et al.*, 1998], the TAG hydrothermal complex on the Mid-Atlantic Ridge [*Al-Hanbali et al.*, 2001], and the MESO zone in the central Indian Ocean [*Halbach et al.*, 2002].

[32] Silicified filamentous microbes found in the MESO zone in the central Indian Ocean are formed of aligned opal-A spheres (2–50 μm diameter) that are pierced by a central canal, <0.2 mm in diameter [e.g., *Herzig et al.*, 1988, Figure 5; *Stüben et al.*, 1994, Figures 5a and 5b; *Halbach et al.*, 2002, Figure 5]. *Al-Hanbali et al.* [2001, Figure 2] described half spheroidal structures, 2–3 μm in diameter, that formed clusters and chains that resembled bacteria colonies. In some deep-sea vent deposits, filamentous microbes were encased with iron hydroxide prior to being encrusted by opal-A [*Halbach et al.*, 2002, Figures 2b and 2c].

[33] Filamentous structures are commonly found in Fe oxides and oxyhydroxides around hydrothermal vents [e.g., *Alt*, 1988; *Juniper and Fouquet*, 1988; *Hekinian et al.*, 1993; *Binns et al.*, 1993; *Bogdanov et al.*, 1997; *Iizasa et al.*, 1998; *Fortin et al.*, 1998; *Boyd and Scott*, 2001; *Little et al.*, 2004; *Emerson et al.*, 2007]. SEM analyses typically reveal sinuous, apparently branching or bundled filaments that are 5–15 μm long and 0.8–2.0 μm wide. Stalk-like structures, formed mainly of amorphous iron oxyhydroxide are commonly associated with the filaments. Such structures have typically been allied with *Leptothrix* or *Gallionella* even though they have not been conclusively identified through culturing or molecular analysis [*Little et al.*, 2004], largely because of the lack of organic carbon or preserved cells in these structures [e.g., *Boyd and Scott*, 2001; *Little et al.*, 2004]. *Emerson and Moyer* [2002] did, however, culture

Figure 4. SEM photomicrographs of silicified microbes, sample B from depth of ~165 m (Figure 1b). (a) General view of silicified microbial mats. (b, c) Enlarged views of microbes forming mat shown in Figure 4a. (d) Traverse cross section through filamentous microbe showing core formed of opal-A encased by outer layer formed of reticulate Fe-rich precipitates. (e) Filamentous microbe encased in reticulate Fe-rich precipitates. (f) Enlarged view of end of filamentous microbe, from Figure 4e, showing open lumen surrounded by reticulate Fe-rich precipitates. (g) Substrate covered with silicified microbes and opal-A spheres. (h) Enlarged view of substrate shown in Figure 4g. (i) Silicified filamentous microbes and scattered opal-A spheres. (j, k) Silicified filamentous microbes. (l) Traverse cross section through filamentous microbe showing open lumen and thin silicified wall. Note opal-A spheres on surrounding substrates.

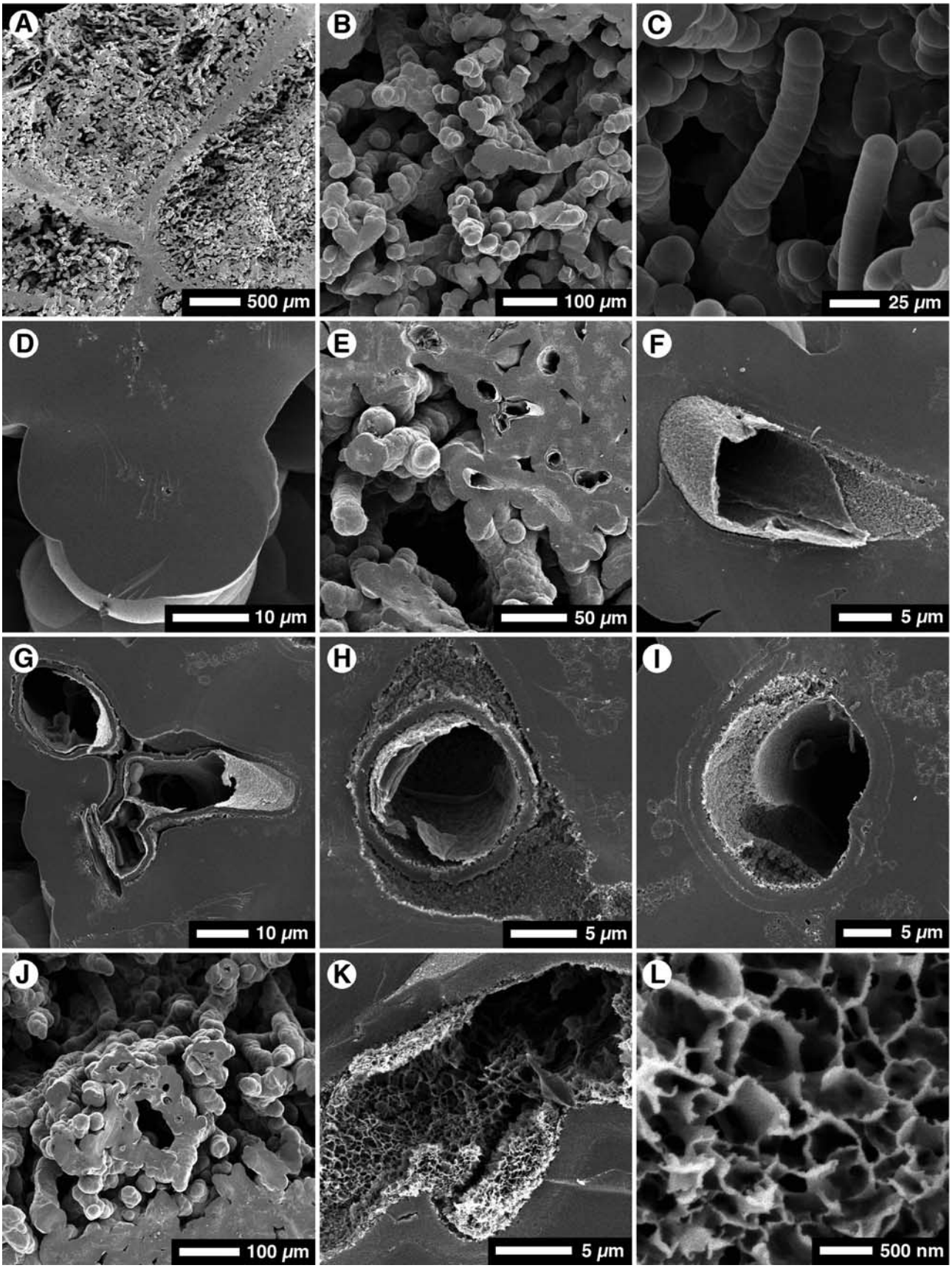
A
500 μm
B
100 μm
C
25 μm
D
10 μm
E
50 μm
F
5 μm
G
10 μm
H
5 μm
I
5 μm
J
100 μm
K
5 μm
L
500 nm

Figure 5

a novel strain of bacterium from the Loihi seamount and *Emerson et al.* [2007], through molecular analysis, showed that two strains of microbes from that site belonged to the Proteobacteria. These microbes, assigned to the new genus *Mariprofundus,* are obligate, lithotropic Fe-oxidizing bacteria [*Emerson et al.*, 2007].

[34] The well-preserved mineralized microbes from Giggenbach volcano include at least four different morphotypes (Figures 3–5). Although the style of silicification is similar to that seen in the silicified filamentous microbes described by *Herzig et al.* [1988], *Stüben et al.* [1994], *Al-Hanbali et al.* [2001], and *Halbach et al.* [2002], it is impossible to determine if the original microbes were the same in all cases. As might be expected, the silicified filamentous microbes from the Giggenbach volcano differ from those microbes that have been preserved in Fe oxides and oxyhydroxides at other seamounts. It is unclear, however, if this merely reflects the style of preservation or if the original microbes were different. The latter seems reasonable given the differences in the chemistry of the hydrothermal fluids that must have existed in the iron-precipitating as opposed to the Si-precipitating sites.

7. Discussion

[35] By virtue of their soft body nature, microbe silicification is a balance between the rate of organic decay and the rate of opal-A replacement and/or encrustation. Microbes will only maintain their three-dimensional form if their tissue is replaced and/or encased before it decays [e.g., *Oehler and Schopf*, 1971; *Oehler*, 1976a, 1976b; *Francis et al.*, 1978; *Bartley*, 1996; *Phoenix and Konhauser*, 1999]. In terrestrial settings, complete decay and loss of microbes can occur within a few days of their death [*Bartley*, 1996]. Indeed, where the water T is >20°C, organic material usually decays before it is replaced by silica [*Walter et al.*, 1998]. The rate of decay of microbes around submarine vents is unknown. At terrestrial hot springs, silicification of microbes commonly begins while they are alive [*Walter*, 1976; *Cassie and Cooper*, 1989; *Schultze-Lam et al.*, 1995; *Jones et al.*, 2001c]. Whether or not this also happens with microbes growing around oceanic vents, such as those associated with Giggenbach volcano, is unknown. Nevertheless, the three-dimensional form of the Giggenbach microbes and preservation of mats formed of loosely but complexly intertwined filamentous microbes imply rapid in situ silicification. This assertion is also supported by the fact that some of the samples were also soft when first collected.

[36] Silicification of microbes, irrespective of their setting, requires the presence of nucleation sites and the steady delivery of solute to those nucleation sites. Many studies have shown that ligands (e.g., hyroxyl groups) on the surfaces of the microbes provide the nucleation sites for silica precipitation [e.g., *Ferris et al.*, 1986; *Schultze-Lam et al.*, 1995; *Konhauser and Ferris*, 1996; *Konhauser et al.*, 2004; *Konhauser*, 2007]. Nevertheless, experimental work seems to indicate that some microbes are more favorably disposed to silicification than others [e.g., *Oehler*, 1976a; *Westall et al.*, 1995; *Toporski et al.*, 2002].

[37] Continued precipitation of opal-A depends on the availability of fluids that are supersaturated with respect to opal-A and their delivery to nucleation sites. The SiO_2 content of hydrothermal fluids expelled from terrestrial springs with high enthalpy is commonly between 200 ppm (e.g., Pohutu, New Zealand [*Jones et al.*, 2001b, Table 1]) and 500 ppm (e.g., Geysir, Iceland [*Jones et al.*, 2007, Table 1]). Nevertheless, precipitation of opal-A is usually achieved only after the supersaturated waters have undergone cooling, evaporation, or a change in pH [e.g., *White et al.*, 1956; *Rimstidt and Cole*, 1983; *Fournier*, 1985; *Renaut and Owen*, 1988; *White et al.*, 1988; *Jones et al.*, 1998]. Hydrothermal fluids expelled from submarine vents commonly contain ~500 ppm SiO_2 [e.g., *Tivey and Delaney*, 1986], usually as a result of seawater-basalt interactions at elevated temperature [e.g., *Edmond*, 1980; *Mottl*, 1983]. By comparison, the host rocks of the Giggenbach hydrothermal system have more silica-rich compositions, such as dacite. At the marker 10 vent site at Giggenbach (Figure 2c), diffuse fluids of 72°C have near-neutral pH (6.3 to 6.6), low total gases (4–5 mM/L) including low H_2S ($\leq$100 μM/L), and contain relatively few metals (e.g., 0.5 to 9.0 μM/L for both Fe and Mn). The highest dissolved SiO_2 concentration recorded was 1034 μM/L (D. A. Butterfield, personal communication, 2007), in keeping with the SiO_2-dominant matrix of the nearby chimneys.

[38] *Janecky and Shanks* [1984] showed that amorphous silica will not precipitate if the temperature decrease of the fluid is due solely to simple mixing with seawater because "...the mixing line of such a fluid does not intersect the saturation curve for amorphous silica" [*Stüben et al.*, 1994, p. 290]. In other words, the dilution of the thermal fluids by seawater may override the effects of rapid cooling on the silica saturation levels. Opal-A may precipitate if additional cooling is achieved by conductive heat removal [*Tivey and Delaney*, 1986; *Alt*, 1988; *Hannington and Scott*, 1988; *Herzig et al.*, 1988; *Stüben et al.*, 1994; *Halbach et al.*, 2002]. Interestingly, *Tivey et al.* [1995] argued that microbial mats might promote conductive cooling as they prevent, or slow down, mixing between the hydrothermal fluids and seawater. *Renaut et al.* [2002] used similar arguments to explain silica precipitation around sublacustrine thermal vents. The silica concentration for the marker

Figure 5. SEM photomicrographs of silicified microbes, sample C from depth of ~160 m (Figure 1b). (a) General view of silicified microbial mats and opal-A sheets. (b) Enlarged view of interwoven silicified filamentous microbes. (c) Silicified filamentous microbe. (d) Transverse cross section through silicified filamentous microbe showing minute opening in core that may be part of original microbe. (e) Group of large filamentous microbes, lined with Fe-rich precipitate and encased with opal-A. (f) Enlarged view from Figure 5F showing Fe-rich precipitate lining open lumen of a filamentous microbe. (g–i) Large diameter filamentous microbes, each lined with Fe-rich precipitate that commonly appears to be formed of two layers. (j) Group of filamentous microbes with open lumens lined with reticulate Fe-rich precipitate. (k–l) Fe-rich reticulate precipitate lining walls of open lumens in filamentous microbes.

10 vent fluids equates to a temperature of ~113°C prior to mixing with ambient seawater (D. A. Butterfield, personal communication, 2007). Irrespective of the mechanism, the coatings of opal-A around the microbes clearly show that solutes supersaturated with respect to opal-A were actively infusing the microbial mats.

[39] The silicified microbes from Giggenbach are morphologically alike many of the silicified microbes found in opal-A deposits that have formed around modern terrestrial hot springs [e.g., *Weed*, 1889a, 1889b; *Cady and Farmer*, 1996; *Jones et al.*, 1997, 2001a, 2001c, 2004b]. Likewise, the Giggenbach microbes preserved in the Fe-rich precipitates are akin to those found in Fe-rich precipitates that are associated with modern terrestrial hot springs. The Fe hydroxide filaments illustrated by *Halbach et al.* [2002, Figures 2b and 2c], for example, are very similar to the filamentous microbes preserved in hydrous ferric oxides found in the acidic waters of Orange Spring on the North Island of New Zealand [*Jones and Renaut*, 2007, Figures 2e–2g]. Similarly, the reticulate Fe-rich precipitates associated with some microbes from Giggenbach volcano (Figures 5k and 5l) are comparable to reticulate precipitates found in hot spring deposits associated with Loburu at Lake Bogoria in Kenya [*Jones and Renaut*, 1996, Figures 2f–2l], the Waikite hot springs on the North Island of New Zealand [*Jones and Renaut*, 1996, Figure 4c], and the Tokaanu geyser vent on the North Island of New Zealand [*Jones et al.*, 2003, Figures 6a–6g]. Filamentous microbes from Tokaanu, for example, are covered with a reticulate coating that appears to be morphologically identical to that found around some of the filamentous microbes from Giggenbach.

[40] The similarity between the styles of microbial mineralization associated with submarine vents and terrestrial springs indicate that microbe mineralization is independent of environmental settings and is simply controlled by the availability of nucleation sites and supply of a solute that is supersaturated with respect to a particular mineral phase. Thus, if the ligands on the microbe surfaces provide appropriate nucleation sites, various minerals including oxides, silicates, carbonates, and sulfides will form [e.g., *Beveridge*, 1981; *Mullen et al.*, 1989; *Fortin and Beveridge*, 1997; *Fortin et al.*, 1997; *Fortin et al.*, 1998]. Furthermore, it also seems that the style of such precipitates is independent of the habitat. Silicification of microbes, for example, involves the precipitation of opal-A microspheres that coat or encase the host microbe, irrespective of their location on land or on the seafloor. Likewise, the multiple episodes of opal-A microspheres evident on some of the filamentous microbes from locality B on Giggenbach volcano (Figure 5i) are directly comparable to the multiple episodes of opal-A microspheres found on microbes from Iodine Pool [*Jones et al.*, 2004a, Figures 8h and 9] a terrestrial hot spring on the North Island of New Zealand.

8. Conclusions

[41] Analysis of mineralized microbes collected 160–180 m below sea level in the deeper part of the photic zone of the submarine Giggenbach submarine volcano has yielded the following conclusions.

[42] 1. The microbes were preserved through silicification and by entombment in reticulate Fe-rich precipitates.

[43] 2. The general morphology, consistency in size and shape, and the presence of features akin to known microbial structures (e.g., septa, sheath) points to a biological origin as opposed to abiogenic precipitates.

[44] 3. Preservation of the three-dimensional forms of the microbes indicates that mineralization was probably rapid as in many terrestrial hot spring systems.

[45] 4. In the absence of rDNA analysis, identification of the mineralized microbes in terms of extant taxa is problematical. This situation common to most of the mineralized microbes that have been described from submarine hydrothermal vents.

[46] 5. The mineralization styles of the Giggenbach microbes are the same as those associated with mineralized microbes found in terrestrial hot spring deposits in New Zealand, Kenya, Iceland and Yellowstone: such similarities exist despite the vastly different environmental settings.

[47] **Acknowledgments.** The samples used in this study were collected during the 2002 NZAPLUME II and 2005 NZASRoF cruises. We thank the captain and crew of the R/V *Tangaroa* and R/V *Ka'imikai-o-Kanaloa* and the pilots and support staff of the *Pisces V* submersible for providing a safe working environment and for the collection of our samples. We also thank Ian Wright of NIWA for supplying the bathymetric data for Giggenbach volcano as part of the NZAPLUME II survey. We are also indebted to the Natural Sciences and Engineering Research Council of Canada Discovery grant A6090 to Jones and RG 629-03 to Renaut that supported examination of the samples, Matthew Stott (GNS, Wairakei), who undertook DNA analyses of the samples, and George Braybrook, University of Alberta, who took the SEM images used in this study. This research was also supported by the New Zealand Foundation for Research, Science and Technology (FRST) grant C05X0406. We are indebted to two anonymous reviewers for their critical comments on an earlier version of this manuscript.

References

Al-Hanbali, H. S., S. J. Sowerby, and N. G. Holm (2001), Biogenicity of silicified microbes from a hydrothermal system: Relevance to the search for evidence of life on earth and other planets, *Earth Planet. Sci. Lett.*, *191*, 213–218, doi:10.1016/S0012-821X(01)00421-6.

Alt, J. C. (1988), Hydrothermal oxide and nontronite deposits on seamounts in the eastern Pacific, *Mar. Geol.*, *81*, 227–239, doi:10.1016/0025-3227(88)90029-1.

Bartley, J. K. (1996), Actualistic taphonomy of cyanobacteria: Implications for the Precambrian fossil record, *Palaios*, *11*, 571–586, doi:10.2307/3515192.

Beveridge, T. J. (1981), Ultrastructure, chemistry and function of the bacterial wall, *Int. Rev. Cytol.*, *72*, 229–317, doi:10.1016/S0074-7696(08)61198-5.

Binns, R. A., et al. (1993), Hydrothermal oxide and gold-rich sulfide deposits of Franklin seamount, western Woodlark Basin, Papua New Guinea, *Econ. Geol.*, *88*, 2122–2153.

Bogdanov, Y. A., A. P. Lizitzin, R. A. Binns, A. I. Gorshov, E. G. Gurvich, V. A. Dritz, G. A. Dubinina, O. Y. Bogdanova, A. V. Sivtsov, and V. M. Kuptsov (1997), Low-temperature hydrothermal deposits of Franklin Seamount, Woodlark Basin, Papua New Guinea, *Mar. Geol.*, *142*, 99–117, doi:10.1016/S0025-3227(97)00043-1.

Boyd, T. D., and S. D. Scott (2001), Microbial and hydrothermal aspects of ferric oxyhydroxides and ferrosic hydroxides: The example of Franklin Seamount, western Woodlark Basin, Papua New Guinea, *Geochem. Trans.*, *7*, doi:10.1039/b105277m.

Cady, S. L., and J. D. Farmer (1996), Fossilization processes in siliceous thermal springs: Trends in preservation along thermal gradients, in *Evolution of Hydrothermal Ecosystems on Earth (and Mars?)*, edited by G. R. Bock and J. A. Goode, p. 150–173, Ciba Foundation Symposium, John Wiley, Chichester, U.K.

Canet, C., R. M. Prol-Ledesma, I. Torres-Alvarado, H. A. Gilg, R. E. Villanueva, and R. Lozano-Santa Cruz (2005), Silica-carbonate stromatolites, related to coastal hydrothermal venting in Bahía, Baja California Sur, Mexico, *Sediment. Geol.*, *174*, 97–113, doi:10.1016/j.sedgeo.2004.12.001.

Cassie, V., and R. C. Cooper (1989), Algae of New Zealand thermal areas, *Bibl. Phycol.*, *38*, 1–159.

de Ronde, C. E. J., E. T. Baker, G. J. Massoth, J. E. Lupton, I. C. Wright, R. A. Feely, and R. G. Greene (2001), Intra-oceanic subduction-related hydrothermal venting, Kermadec volcanic arc, New Zealand, *Earth Planet. Sci. Lett.*, *193*, 359–369, doi:10.1016/S0012-821X(01)00534-9.

de Ronde, C. E. J., G. J. Massoth, E. T. Baker, and J. E. Lupton (2003), Submarine hydrothermal venting related to volcanic arcs, in *Volcanic, Geothermal, and Ore-forming Fluids: Rulers and Witnesses of Processes Within the Earth*, edited by S. F. Simmons and I. Graham, *Spec. Publ. Soc. Econ. Geol.*, 10, 91–110.

de Ronde, C. E. J., et al. (2005), Evolution of a submarine magmatic-hydrothermal system: Brothers volcano, southern Kermadec arc, New Zealand, *Econ. Geol.*, *100*, 1097–1133, doi:10.2113/100.6.1097.

de Ronde, C. E. J., et al. (2007), Submarine hydrothermal activity along the mid-Kermadec Arc, New Zealand: Large-scale effects on venting, *Geochem. Geophys. Geosyst.*, *8*, Q07007, doi:10.1029/2006GC001495.

Edmond, J. M. (1980), The chemistry of the 350°C hot springs at 21°N on the East Pacific Rise, *Eos Trans. AGU*, *68*, 992.

Emerson, D., and C. L. Moyer (2002), Neotrophilic Fe-oxidizing bacteria are abundant at the Loihi Seamount hydrothermal vents and play a major role in Fe oxide deposition, *Appl. Environ. Microbiol.*, *68*, 3085–3093, doi:10.1128/AEM.68.6.3085-3093.2002.

Emerson, D., J. A. Rentz, T. G. Lilburn, R. E. Davis, H. Aldrich, C. Chan, and C. L. Moyer (2007), A novel lineage of Proteobacteria involved in formation of marine Fe-oxidizing microbial mat communities, *PLoS One*, *2*(8), e667, doi:10.1371/journal.pone.0000667.

Ferris, F. G., T. J. Beveridge, and W. S. Fyfe (1986), Iron-silica crystallite nucleation by bacteria in geothermal sediment, *Nature*, *320*, 609–611, doi:10.1038/320609a0.

Fortin, D., and T. J. Beveridge (1997), Role of the bacterium *Thiobacillus* in the formation of silicates in acidic mine tailings, *Chem. Geol.*, *141*, 235–250, doi:10.1016/S0009-2541(97)00069-7.

Fortin, D., F. G. Ferris, and T. J. Beveridge (1997), Surface-mediated mineral development by bacteria, in *Geomicrobiology: Interactions Between Microbes and Minerals*, edited by J. F. Banfield and K. H. Nealson, pp. 161–180, Mineral. Soc. of Am., Blacksburg, Va.

Fortin, D., F. G. Ferris, and S. D. Scott (1998), Formation of Fe-silicates and Fe-oxides on bacterial surfaces in samples collected near hydrothermal vents on the Southern Explorer Ridge in the northeast Pacific Ocean, *Am. Mineral.*, *83*, 1399–1408.

Fournier, R. O. (1985), The behavior of silica in hydrothermal solutions, *Rev. Econ. Geol.*, *2*, 45–61.

Francis, S., L. Margulis, and E. S. Barghoorn (1978), On the experimental silicification of microorganisms. II. On the time of appearance of eukaryotic organisms in the fossil record, *Precambrian Res.*, *6*, 65–100, doi:10.1016/0301-9268(78)90055-4.

García-Ruiz, J. M., A. M. Carnerup, A. G. Christy, N. J. Welham, and S. T. Hyde (2002), Morphology: An ambiguous indicator of biogenicity, *Astrobiology*, *2*, 353–369, doi:10.1089/153110702762027925.

García-Ruiz, J. M., S. T. Hyde, A. M. Carnerup, A. G. Christy, M. J. Van Krandendonk, and N. J. Welham (2003), Self-assembled silica-carbonate structures and detection of ancient microfossils, *Science*, *302*, 1194–1197, doi:10.1126/science.1090163.

Halbach, M., P. Halbach, and V. Lüders (2002), Sulfide-impregnated and pure silica precipitates of hydrothermal origin from the central Indian Ocean, *Chem. Geol.*, *182*, 357–375, doi:10.1016/S0009-2541(01)00323-0.

Hannington, M. D., and S. D. Scott (1988), Mineralogy and geochemistry of a hydrothermal silica-sulfide-sulfate spire in the caldera of Axial Seamount, Juan de Fuca Ridge, *Can. Mineral.*, *26*, 603–625.

Hekinian, R., M. Hoffert, P. Larqué, J. L. Cheminée, P. Stoffers, and D. Bideau (1993), Hydrothermal Fe and Si oxyhydroxide deposits from South Pacific intraplate volcanoes and East Pacific Rise axial and off-axial regions, *Econ. Geol.*, *88*, 2099–2121.

Herzig, P. M., K. P. Becker, P. Stoffers, H. Bäcker, and N. Blum (1988), Hydrothermal silica chimney fields in the Galapagos Spreading Center at 86°W, *Earth Planet. Sci. Lett.*, *89*, 261–272, doi:10.1016/0012-821X(88)90115-X.

Iizasa, K., K. Kawasaki, K. Maeda, T. Matsumoto, N. Saito, and K. Hirai (1998), Hydrothermal sulfide-bearing Fe-Si oxyhydroxide deposits from the Coriolis troughs, Vanuatu backarc, southwestern Pacific, *Mar. Geol.*, *145*, 1–21, doi:10.1016/S0025-3227(97)00112-6.

Iler, R. K. (1979), *The Chemistry of Silica*, 866 pp., John Wiley, New York.

Janecky, D. R., and W. C. Shanks (1984), Formation of massive sulfide deposits on oceanic ridge crests: Incremental reaction models for mixing between hydrothermal solutions and seawater, *Geochim. Cosmochim. Acta*, *48*, 2723–2738, doi:10.1016/0016-7037(84)90319-3.

Jones, B., and R. W. Renaut (1996), Influence of thermophilic bacteria on calcite and silica precipitation in hot springs with water temperatures above 90°C: Evidence from Kenya and New Zealand, *Can. J. Earth Sci.*, *33*, 72–83.

Jones, B., and R. W. Renaut (2007), Selective mineralization of microbes in Fe-rich precipitates (jarosite, hydrous ferric oxides) from acid hot springs in the Waiotapu geothermal area, North Island, New Zealand, *Sediment. Geol.*, *194*, 77–98, doi:10.1016/j.sedgeo.2006.05.025.

Jones, B., R. W. Renaut, and M. R. Rosen (1997), Biogenicity of silica precipitation around geysers and hot-spring vents, North Island, New Zealand, *J. Sediment. Res.*, *67*, 88–104.

Jones, B., R. W. Renaut, and M. R. Rosen (1998), Microbial biofacies in hot-spring sinters: A model based on Ohaaki Pool, North Island, New Zealand, *J. Sediment. Res.*, *68*, 413–434.

Jones, B., R. W. Renaut, and M. R. Rosen (2001a), Biogenicity of gold- and silver-bearing siliceous sinters forming in hot (75°C) anaerobic spring-waters of Champagne Pool, North Island, New Zealand, *J. Geol. Soc.*, *158*, 895–911, doi:10.1144/0016-764900-131.

Jones, B., R. W. Renaut, and M. R. Rosen (2001b), Microbial construction of siliceous stalactites at geysers and hot springs: Examples from the Whakarewarewa geothermal area, North Island, New Zealand, *Palaios*, *16*, 73–94.

Jones, B., R. W. Renaut, and M. R. Rosen (2001c), Taphonomy of silicified filamentous microbes in modern geothermal sinters—Implications for identification, *Palaios*, *16*, 580–592.

Jones, B., R. W. Renaut, and M. R. Rosen (2003), Silicified microbes in a geyser mound: The enigma of low-temperature cyanobacteria in a high-temperature setting, *Palaios*, *18*, 87–109, doi:10.1669/0883-1351(2003)18<87:SMIAGM>2.0.CO;2.

Jones, B., K. O. Konhauser, R. W. Renaut, and R. Wheeler (2004a), Microbial silicification in Iodine Pool, Waimangu Geothermal area, North Island, New Zealand: Implications for recognition and identification of ancient silicified microbes, *J. Geol. Soc.*, *161*, 983–993, doi:10.1144/0016-764903-172.

Jones, B., R. W. Renaut, and M. R. Rosen (2004b), Taxonomic fidelity of silicified microbes from hot spring systems in the Taupo Volcanic Zone, North Island, New Zealand, *Trans. R. Soc. Edinburgh Earth Sci.*, *94*, 475–483.

Jones, B., R. W. Renaut, H. Torfason, and B. Owen (2007), The historical development of Geysir, Iceland, *J. Geol. Soc.*, *164*, 1241–1252, doi:10.1144/0016-76492006-178.

Juniper, S. K., and Y. Fouquet (1988), Filamentous iron-silica deposits from modern and ancient hydrothermal sites, *Can. Mineral.*, *26*, 859–870.

Konhauser, K. O. (2007), *Introduction to Geomicrobiology*, Blackwell, Oxford, U.K.

Konhauser, K. O., and F. G. Ferris (1996), Diversity of iron and silica precipitation by microbial mats in hydrothermal waters, Iceland: Implications for Precambrian iron formations, *Geology*, *24*, 323–326, doi:10.1130/0091-7613(1996)024<0323:DOIASP>2.3.CO;2.

Konhauser, K. O., W. S. Fyfe, F. G. Ferris, and T. J. Beveridge (1993), Metal sorption and mineral precipitation by bacteria in two Amazonian river systems, Rio Solimoes and Rio Negro, *Geology*, *21*, 1103–1106, doi:10.1130/0091-7613(1993)021<1103:MSAMPB>2.3.CO;2.

Konhauser, K. O., B. Jones, V. R. Phoenix, F. G. Ferris, and R. W. Renaut (2004), The microbial role in hot spring silicification, *Ambio*, *33*, 552–558, doi:10.1639/0044-7447(2004)033[0552:TMRIHS]2.0.CO;2.

Little, C. T. S., S. E. Glynn, and R. A. Mills (2004), Four hundred and ninety million year record of bacteriogenic iron oxide precipitation at sea-floor hydrothermal vents, *Geomicrobiol. J.*, *21*, 415–429, doi:10.1080/01490450490485845.

Mottl, M. J. (1983), Metabasalts, axial hot springs, and the structure of hydrothermal systems at mid-ocean ridges, *Geol. Soc. Am. Bull.*, *94*, 161–180, doi:10.1130/0016-7606(1983)94<161:MAHSAT>2.0.CO;2.

Mullen, M. D., D. C. Wolf, F. G. Ferris, T. J. Beveridge, C. A. Flemming, and G. W. Bailey (1989), Bacterial sorption of heavy metals, *Appl. Environ. Microbiol.*, *55*, 3143–3149.

Oehler, J. H. (1976a), Experimental studies in Precambrian paleontology: Structural and chemical changes in blue-green algae during simulated fossilization in synthethic chert, *Geol. Soc. Am. Bull.*, *87*, 117–129, doi:10.1130/0016-7606(1976)87<117:ESIPPS>2.0.CO;2.

Oehler, J. H. (1976b), Hydrothermal crystallization of silica gel, *Geol. Soc. Am. Bull.*, *87*, 1143–1152, doi:10.1130/0016-7606(1976)87<1143:HCOSG>2.0.CO;2.

Oehler, L. H., and J. W. Schopf (1971), Artificial microfossils: Experimental studies of permineralization of blue-green algae in silica, *Science*, *174*, 1229–1231, doi:10.1126/science.174.4015.1229.

Phoenix, V. R., and K. O. Konhauser (1999), Photosynthetic controls on the silicification of cyanobacteria, in *Geochemistry of the Earth's Surface*, edited by H. Armannsson, pp. 275–278, A.A. Balkema, Rotterdam, Netherlands.

Phoenix, V. R., K. O. Konhauser, and F. G. Ferris (2003), Experimental study of iron and silica immobilization by bacteria in mixed Fe-Si systems: Implications for microbial silicification in host springs, *Can. J. Earth Sci.*, *40*, 1669–1678, doi:10.1139/e03-044.

Remsen, C. C., J. V. Klump, J. Kaster, R. Paddock, P. Anderson, and J. S. Maki (1990), Hydrothermal springs and gas fumaroles in Yellowstone Lake, Yellowstone National Park, Wyoming, *Natl. Geogr. Res.*, *6*, 509–515.

Renaut, R. W., and R. B. Owen (1988), Opaline cherts associated with sublacustrine hydrothermal springs at Lake Bogoria, Kenya Rift Valley, *Geology*, *16*, 699–702, doi:10.1130/0091-7613(1988)016<0699:OCAWSH>2.3.CO;2.

Renaut, R. W., B. Jones, J.-J. Tiercelin, and C. Tarits (2002), Sublacustrine precipitation of hydrothermal silica in rift lakes: Evidence from Lake Baringo, central Kenya Rift Valley, *Sediment. Geol.*, *148*, 235–257, doi:10.1016/S0037-0738(01)00220-2.

Reysenbach, A.-L., and S. L. Cady (2001), Microbiology of ancient and modern hydrothermal systems, *Trends Microbiol.*, *9*, 79–86, doi:10.1016/S0966-842X(00)01921-1.

Rimstidt, J. D., and D. R. Cole (1983), Geothermal mineralization I: The mechanism of formation of the Beowawe, Nevada, siliceous sinter deposit, *Am. J. Sci.*, *283*, 861–875.

Schultze-Lam, S., F. G. Ferris, K. O. Konhauser, and R. G. Wiese (1995), In situ silicification of an Icelandic hot spring microbial mat: Implications for microfossil formation, *Can. J. Earth Sci.*, *32*, 2021–2026.

Stüben, D., N. E. Taibi, G. M. McMurty, J. Scholten, P. Stoffers, and D. Zhang (1994), Growth history of a hydrothermal silica chimney from the Mariana backarc spreading center (southwest Pacific, 18°13′N), *Chem. Geol.*, *113*, 273–296, doi:10.1016/0009-2541(94)90071-X.

Tivey, M. K., and J. R. Delaney (1986), Growth of large sulfide structures on the Endeavour Segment of the Juan de Fuca Ridge, *Earth Planet. Sci. Lett.*, *77*, 303–317, doi:10.1016/0012-821X(86)90142-1.

Tivey, M. K., S. E. Humphies, G. Thompson, M. D. Hannington, and P. A. Rona (1995), Deducting patterns of fluid flow and mixing within the active TAG hydrothermal mound, using mineralogical and geochemical data, *J. Geophys. Res.*, *100*, 12,527–12,555, doi:10.1029/95JB00610.

Toporski, J. K. W., A. Steele, F. Westall, K. L. Thomas-Keprta, and D. S. McKay (2002), The simulated silicification of bacteria—New clues to the modes and timing of bacterial preservation and implications for the search for extraterrestrial microfossils, *Astrobiology*, *2*, 1–26, doi:10.1089/153110702753621312.

Urrutia, M. M., and T. J. Beveridge (1994), Formation of fine-grained metal and silicate precipitates on a bacterial surface (*Bacillus subtilis*), *Chem. Geol.*, *116*, 261–280, doi:10.1016/0009-2541(94)90018-3.

Walter, M. R. (1976), Geyserites of Yellowstone National Park: An example of abiogenic stromatolites, in *Stromatolites, Dev. Sediment.*, vol. 20, edited by M. R. Walter, pp. 87–112, Elsevier, Amsterdam.

Walter, M. R., S. McLoughlin, A. N. Drinnan, and J. D. Farmer (1998), Palaeontology of Devonian thermal spring deposits, Drummond Basin, Australia, *Alcheringa*, *22*, 285–314.

Weed, W. H. (1889a), On the formation of siliceous sinter by the vegetation of thermal springs, *Am. J. Sci.*, *37*, 351–359.

Weed, W. H. (1889b), The vegetation of hot springs, *Am. Nat.*, *23*, 394–398, doi:10.1086/274927.

Weed, W. H. (1890), Geysers, *Sch. Mines Q. Columbia Coll.*, *11*, 289–306.

Westall, F., L. Boni, and E. Guerzoni (1995), The experimental silicification of microorganisms, *Palaeontology, 38*, 495–528.

White, D. E., W. W. Brannock, and K. J. Murata (1956), Silica in hot-spring waters, *Geochim. Cosmochim. Acta*, *10*, 27–59, doi:10.1016/0016-7037(56)90010-2.

White, D. E., R. A. Hutchinson, and T. E. C. Keith (1988), The geology and remarkable thermal activity of Norris Geyser Basin, Yellowstone National Park, Wyoming, *U.S. Geol. Surv. Prof. Pap.*, 1456, 84 pp.

Yee, N., V. R. Phoenix, K. O. Konhauser, L. G. Benning, and F. G. Ferris (2003), The effect of cyanobacteria on silica precipitation at neutral pH: Implications for bacterial silicification in geothermal hot springs, *Chem. Geol.*, *199*, 83–90, doi:10.1016/S0009-2541(03)00120-7.

C. E. J. de Ronde, GNS Science, P.O. Box 30-368, Lower Hutt 6315, New Zealand.

B. Jones, Department of Earth and Atmospheric Sciences, University of Alberta, Edmonton, AB T6G 2E3, Canada. (brian.jones@ualberta.ca)

R. W. Renaut, Department of Geological Sciences, University of Saskatchewan, Saskatoon, SK, S7N 5E2, Canada.